JKAU: Eng. Sci., **vol. 16 no. 1**, pp. 147-163 (2005 A.D./1426 A.H.)

Stress Fields For Sharp Notches in Pressure-Sensitive Materials Under Plane-Stress Conditions

ABDULHAMID AL-ABDULJABBAR
Riyadh College of Technology, Riyadh, Saudi Arabia
E-mail: jabbar@gotevot.edu.sa

ABSTRACT. Fully-developed plastic stress fields around sharp wedge-shaped notches of perfectly-plastic pressure-sensitive materials are investigated for plane-stress case and symmetric tensile loading conditions. The pressure-sensitive yielding behavior of the material is represented by the Drucker-Prager yield criterion. Using equilibrium equations, boundary conditions, and the yield criterion, closed-form expressions for stress fields are derived. The analysis covers the gradual change in the notch angle starting from the limiting case of a pure horizontal crack, the solution of which is compared with published literature. Effects of notch geometry and pressure sensitivity on stress fields are examined by considering different specimen geometries, as well as different levels of pressure sensitivity. Results indicate that while stress values directly ahead of the notch-tip are not affected, the extent of stress sector at notch front is reduced, thereby causing increase in the radial stress value around the notch. As the pressure sensitivity increases the reduction of the stress sector directly ahead of the notch tip is more evident. Also, for high pressure sensitivity values, introduction of the notch angle reduces the variation of the stress levels. Results obtained from the analysis are useful for design of structural components.

KEYWORDS: Crack tip, stress fields, notch, plane stress, pressure-sensitive yielding.

1. Introduction

Dependence of material yield and ultimate strength on the hydrostatic stress state, which is known as pressure sensitivity, is evident in many classes of engineering materials such as polymers, according to Sternstein and Ongchin, [1], Spitzig and Richmond, [2], and Kinloch and Young, [3]; cast irons, and, to

a lesser degree, in some steels as reported by Dong *et al.* [4] and Richmond and Spitzig [5], respectively. Phase transformation in some ceramic materials is highly dependent on pressure sensitivity, as reported by Yu and Shetty [6] and Chen [7].

The effect of pressure sensitivity on the yield behavior can be accounted for using the simple form of the Drucker-Prager yield criterion. In this criterion, a generalized form of the yield stress is expressed as a function of the tensile yield stress and the hydrostatic stress using a pressure sensitivity factor. The latter is a material mechanical property dependent on the difference between yield stresses in tension and compression. Experimental investigations referenced above, reported different values of pressure sensitivity factor for different materials. The pressure sensitivity factor ranges from quite a low value 0.064 for some steels [5] to a modest range of 0.1 ~ 0.25 for polymers [2, 3] and 0.22 for cast irons [4], to a large value up to 0.93 for zirconia-containing phase-transformation ceramics [6, 7].

Crack initiation and growth depend largely on the stress and deformation fields around the tip. Therefore, investigation of stress fields near the tip is important to relate the continuum stress analysis to micromechanical failure mechanisms. Rice and Rosengren [8] and Hutchinson [9] developed asymptotic crack-tip stress and strain fields for von-Mises materials. Solutions of crack-tip fields for perfectly-plastic and hardening pressure-sensitive materials for the plane strain case were developed by Li and Pan [10]; and solutions for the plane stress case were presented by Li and Pan [11] and Li [12]. Al-Abduljabbar and Pan [13] extended the crack-tip stress fields solution for the plane strain case for wedge-shaped sharp and blunted notches and presented the combined effects of notch geometry and pressure sensitivity on the stress fields. It was shown in their work that notch geometry has strong effect on stress fields around notch tip.

Building on the aforementioned literature on the plane stress case, and using a similar approach to the one used for the plane strain case, this work aims to determine the solution for notch-tip stress fields for pressure sensitive materials under symmetric tensile loading for the plane stress case, to include effects of geometry on stress fields.

Material pressure-sensitivity will be represented by the Drucker-Prager yield criterion. Starting with equilibrium equations, boundary conditions, and the yield criterion, closed-form expressions for stress fields will be derived. The analysis will include the gradual change in the notch angle starting from the limiting case of a pure horizontal crack, where the notch angle is zero. This case will be considered as the limiting case for the analysis. Since the results

for such case are available in the literature, the results obtained here will be compared with published work for pure horizontal crack.

2. Notch-Tip Fields

Consider a sharp notch with a total wedge angle 2γ as shown in Fig. 1, where both Cartesian and polar coordinates are centered at the notch tip. Under plane stress conditions, the material is subjected to symmetric tensile loading and fully plastic loading is assumed. The general stress distribution can be obtained based on the classical analysis of the problem given in [14]. Li [12] derived the closed form solution of the centered-fan stress sector around a sharp crack for pressure-sensitive materials. In what follows, a closed-form solution for a wedge-shaped notch with the notch angle $\gamma > 0$, is developed. The limiting case of $\gamma = 0$ should correspond to the pure horizontal crack solution.

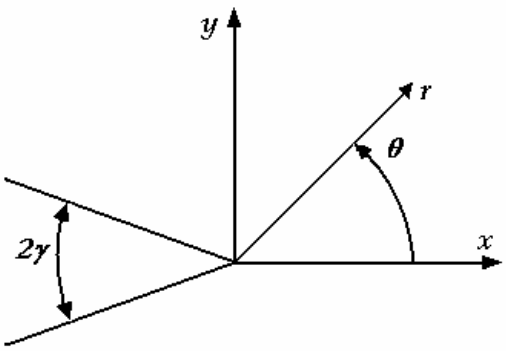

Figure 1: A sharp notch with a total wedge angle 2γ, and coordinate systems centered at the notch tip.

For pressure-sensitive materials, the yield condition can be expressed as a linear function of the effective stress $\bar{\sigma}_e$ and the hydrostatic (mean) stress $\bar{\sigma}_m$ using the pressure sensitivity factor μ as follows

$$f(\bar{\sigma}) = \bar{\sigma}_e + \sqrt{3}\mu\bar{\sigma}_m - \bar{\sigma}_0 = 0 . \tag{1}$$

In Equation $1, \bar{\sigma}_e = (\bar{s}_{ij}\bar{s}_{ij})^{1/2}$, where $\bar{s}_{ij}$ are the deviatoric stress components defined by $\bar{s}_{ij} = \bar{\sigma}_{ij} - \bar{\sigma}_m\delta_{ij}$. Here, $\bar{\sigma}_{ij}$ represent stress components and δ_{ij} is

the Kronecker delta. The summation convention is adopted for repeated indices. The mean stress is defined by the relation $\overline{\sigma}_m = \overline{\sigma}_{kk}/3$.

In polar coordinates system, the yield criterion for rigid perfectly-plastic materials under plane stress conditions takes the form

$$(\sigma_{rr}^2+\sigma_{\theta\theta}^2-\sigma_{rr}\sigma_{\theta\theta}+3\sigma_{r\theta}^2)^{1/2}+\frac{\mu}{\sqrt{3}}(\sigma_{rr}+\sigma_{\theta\theta})=1; \tag{2}$$

where the unbarred stress quantities are normalized by the generalized effective stress $\overline{\sigma}_0$. In what follows, all unbarred stress quantities are normalized in the same way.

Equilibrium equations in the polar coordinate system for the plane stress condition, where stresses in the out-of-plane directions are zeros, can be written as follows

$$\frac{\partial\sigma_{rr}}{\partial r}+\frac{1}{r}\frac{\partial\sigma_{r\theta}}{\partial\theta}+\frac{\sigma_{rr}-\sigma_{\theta\theta}}{r}=0, \tag{3}$$

$$\frac{\partial\sigma_{r\theta}}{\partial r}+\frac{1}{r}\frac{\partial\sigma_{\theta\theta}}{\partial\theta}+\frac{2\sigma_{r\theta}}{r}=0. \tag{4}$$

As discussed by Rice [15], for perfectly plastic materials, the stress is bounded as $r\to 0$; from which the quantity $r(\partial\sigma_{ij}/\partial r)$ approaches 0. Therefore, equilibrium equations reduce to

$$\frac{\partial\sigma_{r\theta}}{\partial\theta}+\sigma_{rr}-\sigma_{\theta\theta}=0, \tag{5}$$

$$\frac{\partial\sigma_{\theta\theta}}{\partial\theta}+2\sigma_{r\theta}=0. \tag{6}$$

Defining a symmetric tensor $\widetilde{P}$, such that $P_{ij}=\partial f/\partial\sigma_{ij}$, Rice [14] was able to reduce the equilibrium equations and the differential form of the yield condition into one governing equation for plastic sectors near crack tip as follows

$$\frac{d(\sigma_{11}+\sigma_{22})}{d\theta}P_{rr}=0. \tag{7}$$

where P_{rr} is the *rr* component of the outward normal to the yield surface in the stress space.

Based on Hill's solution [16], Equation 7 gives rise to two possible solutions of the stress fields for the fully- developed plastic region around the

notch tip. The first solution comes from setting the first item in the right hand side of the equation to zero. This solution dictates uniform Cartesian stress components within the region. The second solution comes from setting the second item in the equation, P_{rr} , to zero; which implies that radial lines correspond to one of the two families of characteristics of the field. This gives rise to the centered fan sector.

Hutchinson [14] indicated that a possible solution for this case consists of three distinctive stress sectors. With reference to Fig. 2, symmetry around the *x*-axis allows consideration of only one half of the notch. The region adjacent to the free surface, which is denoted in the figure by CS *I*, is a constant stress sector where Cartesian stress components remain constants. The second region, denoted by CS *II*, is also a constant stress sector, with a discontinuity in the radial stress between the two regions. The third region, which is located directly ahead of the notch tip, is a centered fan sector where the radial lines represent a family of characteristic lines of the hyperbolic stress equations. The initial and boundary conditions will be utilized to invoke the geometry change around the crack tip and obtain expressions for the stress fields.

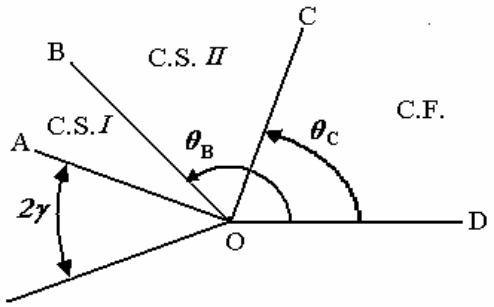

Figure 2: Assembly of notch-tip sectors near a sharp notch tip.

2.1 Constant Stress Sector I

Referring to Fig. 2, the stress-free boundary conditions of the notch surface require that $\sigma_{\theta\theta} = \sigma_{r\theta} = 0$ at $\theta = \pi - \gamma$. Applying the yield condition (Equation 2) at this boundary, we obtain an expression for the radial stress:

$$\sigma_{rr}(\pi-\gamma)=-\frac{\sqrt{3}}{\sqrt{3}-\mu}. \tag{8}$$

With Cartesian stress components ($\sigma_{xx},\sigma_{yy},\sigma_{xy}$) constant in this sector, stress transformation equations are used to obtain the general form of stress fields in the constant stress sector in the polar coordinate system which results the following

$$\begin{aligned}\sigma_{rr}(\theta) &= C + A\cos 2\theta + B\sin 2\theta,\\ \sigma_{\theta\theta}(\theta) &= C - A\cos 2\theta - B\sin 2\theta,\\ \sigma_{r\theta}(\theta) &= -A\sin 2\theta + B\cos 2\theta;\end{aligned} \tag{9}$$

where *A, B* and *C* are constants. Free boundary conditions and Equation 8 are used to evaluate stress components at the boundary. The latter are substituted in the general form of Equation 9, from which stress fields throughout this sector are obtained

$$\begin{aligned}\sigma_{rr}(\theta) &= -\frac{1}{2}\beta[1+\cos 2(\theta+\gamma)],\\ \sigma_{\theta\theta}(\theta) &= -\frac{1}{2}\beta[1-\cos 2(\theta+\gamma)],\\ \sigma_{r\theta}(\theta) &= \frac{1}{2}\beta\sin 2(\theta+\gamma).\end{aligned} \tag{10}$$

In Equation 10, β is a constant related to the pressure sensitivity factor μ by the relation

$$\beta=\frac{\sqrt{3}}{\sqrt{3}-\mu}.$$

2.2 Constant Stress Sector II

Along the border of the two constant stress sectors, which is represented by the angle θ_B, traction continuity requires the continuity of the angular and shear stresses ($\sigma_{\theta\theta}$ and $\sigma_{r\theta}$). The difference in the radial stress values at the border between the two regions, denoted as D (θ_B), can be obtained using the yield condition and the known stress quantities as given by [12]:

$$\sigma_{rr}^{-}-\sigma_{rr}^{+}=\beta D(\theta_B)=$$

$$\frac{3}{3-\mu^2}[4-(3-4\mu^2)\sigma_{\theta\theta}^2(\theta_B)-4(3-\mu^2)\sigma_{r\theta}^2(\theta_B)-4\sqrt{3}\mu\sigma_{\theta\theta}(\theta_B)]^{1/2}. \quad (11)$$

Substituting the stress values of Equation 10 at θ_B into Equation 11, we obtain the expression for the constant *D:*

$$D=\frac{3}{2(3-\mu^2)}[1-\frac{4\mu}{\sqrt{3}}+3\cos 2(\theta_B+\gamma)]. \quad (12)$$

The radial stress can then be determined as

$$\bar{\sigma}_{rr}(\theta_B)=\beta[D-\frac{1}{2}(1+\cos(\theta_B+\gamma)]. \quad (13)$$

From continuity requirements of stress components $\sigma_{\theta\theta}$ and $\sigma_{r\theta}$ along sectors CS *I* and CS *II*, and Equation 13, stress components can be determined at the boundary angle θ_B. Consequently, stress fields within this sector can be determined

$$\begin{aligned}\sigma_{rr}(\theta)&=\beta(D-1)/2+A\cos 2\theta+B\sin 2\theta,\\ \sigma_{\theta\theta}(\theta)&=\beta(D-1)/2-A\cos 2\theta-B\sin 2\theta,\\ \sigma_{r\theta}(\theta)&=-A\sin 2\theta+B\cos 2\theta;\end{aligned} \quad (14)$$

where the constants *A* and *B* are

$$\begin{aligned}A&=\frac{\beta}{2}[D\cos 2\theta_B-\cos 2\gamma]\\ B&=\frac{\beta}{2}[D\sin 2\theta_B+\sin 2\gamma]\end{aligned} \quad (15)$$

Although the form in Equation 14 looks different, both stress solutions in Equations 10 and 14 simplify to those of pure horizontal crack given in [12] when the notch angle is set to zero and the case is reduced to a pure crack problem. This serves as a check for the results presented here.

2.3 Centered Fan Sector

The closed form solution for the centered fan sector for plane stress pressure-sensitive sharp crack fields was developed elsewhere [12]. Since the effect of geometry on this sector is only on the extent of the sector, that is, the value of the angle θ_C; such solution for the stress fields is sufficient for our problem, and it is presented below.

$$\sigma_{rr} = \frac{1}{3-4\mu^2}\left[\frac{3+2\mu^2}{(3-\mu^2)^{1/2}}\cos k\theta - 2\sqrt{3}\mu\right],$$
$$\sigma_{\theta\theta} = \frac{1}{3-4\mu^2}\left[2(3-\mu^2)^{1/2}\cos k\theta - 2\sqrt{3}\mu\right] \tag{16}$$
$$\sigma_{r\theta} = \frac{1}{\left(3-4\mu^2\right)^{1/2}}\sin k\theta;$$

for $\mu < \sqrt{3}/2$;

$$\sigma_{rr} = -\frac{2}{3}\theta^2,$$
$$\sigma_{\theta\theta} = \frac{2}{3}(1-\theta^2), \tag{17}$$
$$\sigma_{r\theta} = \frac{2}{3}\theta;$$

for $\mu = \sqrt{3}/2$; and

$$\sigma_{rr} = \frac{1}{4\mu^2-3}\left[\frac{3+2\mu^2}{(3-\mu^2)^{1/2}}\cosh k\theta + 2\sqrt{3}\mu\right],$$
$$\sigma_{\theta\theta} = \frac{1}{4\mu^2-3}\left[2(3-\mu^2)^{1/2}\cosh k\theta + 2\sqrt{3}\mu\right] \tag{18}$$
$$\sigma_{r\theta} = \frac{1}{\left(4\mu^2-3\right)^{1/2}}\sinh k\theta;$$

for $\mu > \sqrt{3}/2$.

3. Results

In this section, we present the results of the stress fields obtained from the previous section for each region. The extent of each region and stress distributions are presented using pertinent boundary conditions.

3.1 Extent of Sectors

The extent of each sector in the assembly presented is obtained by determination of the two border angles θ_B and θ_C. This can be achieved by invoking the traction continuity conditions at θ_C and matching the angular and

shear stresses from the two adjacent sectors. Hence, Equations 14, 16-18 can be used to get two simultaneous equations for angles θ_B and θ_C

$$\begin{aligned}\sigma_{\theta\theta}^{CF}(\theta_C) &= \beta(D-1)/2 - A\cos 2\theta_C - B\sin 2\theta_C,\\ \sigma_{r\theta}^{CF}(\theta_C) &= -A\sin 2\theta_C + B\cos 2\theta_C.\end{aligned} \tag{19}$$

μ	γ	θ_B	θ_C	Values from [12]	
				θ_B	θ_C
0.00	0.00	151.24	79.84	151.24	79.84
	22.50	137.20	68.35	--	--
	45.00	123.60	59.36	--	--
0.20	0.00	151.14	73.03	151.14	73.03
	22.50	136.43	60.55	--	--
	45.00	121.93	50.01	--	--
0.40	0.00	152.16	67.21	152.16	67.21
	22.50	136.84	54.15	--	--
	45.00	121.62	42.46	--	--
0.70	0.00	155.02	59.08	155.02	59.08
	22.50	138.84	45.65	--	--
	45.00	122.62	32.65	--	--
1.00	0.00	159.09	50.68	159.09	50.68
	22.50	142.04	37.32	--	--
	45.00	124.80	23.24	--	--

Table 1: Numerical values for θ_B and θ_C for different values of μ and γ with comparison of the results of Li, [12].

The superscript "CF" refers to the centered fan sector where the proper form of the stress is used depending on the value of μ. With the constants determined by Equation 10, the material pressure sensitivity given and the notch angle set, the two angles can be solved for using a simple numerical technique. The result is summarized in Table 1. It is worthy to mention that when we compare the values of θ_B and θ_C obtained here for different cases of pressure sensitivities and $\gamma = 0$, with the results of Li [12] for sharp horizontal crack, we find that they match, which validates the solution developed earlier in this work.

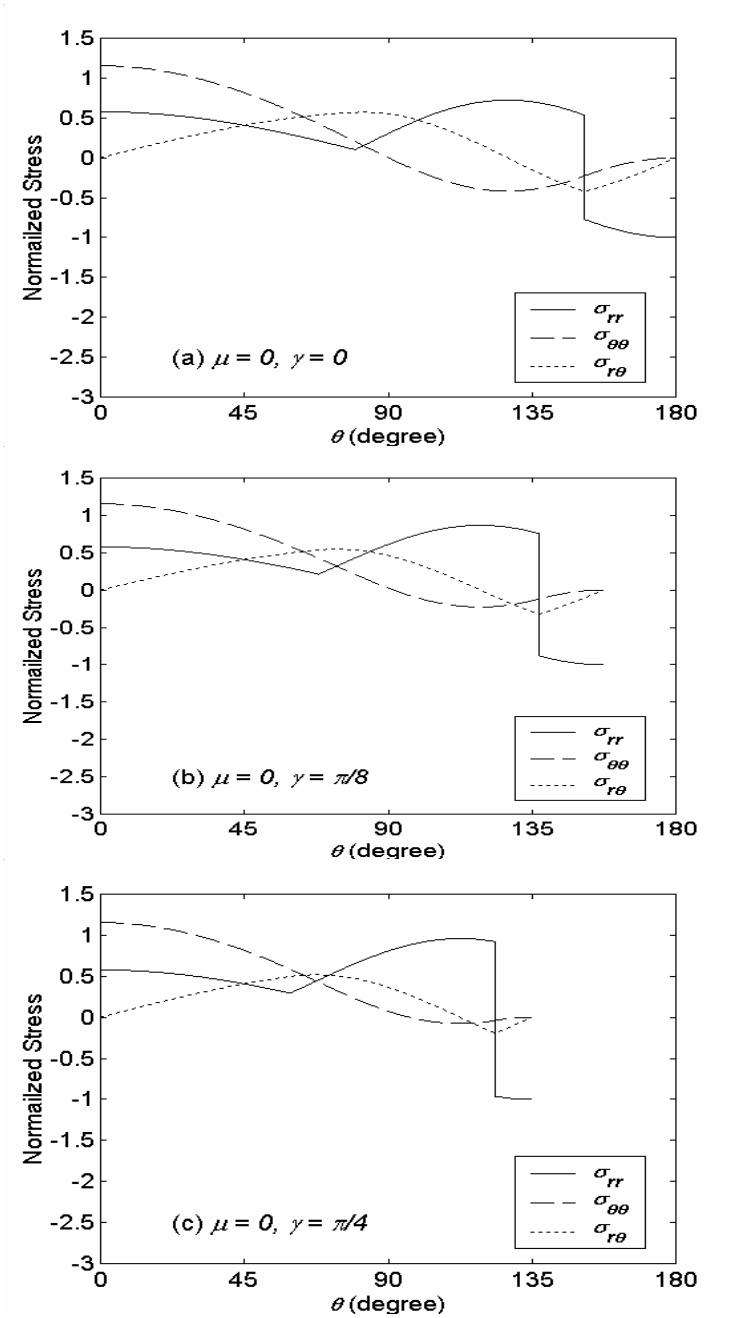

Figure 3: Angular variation of normalized stresses for a sharp notch with μ =0.0 for notch angle values of γ= 0, π/ 8 and π/ 4.

Considering Table 1, we see that for the case of no pressure sensitivity, $\mu =$ 0, the effect of introducing the notch tends to reduce the angular span of all the three sectors in a balanced fashion. However, this initial effect changes as the pressure sensitivity is introduced, at which the balance is shifted into reducing more of the centered fan sector and sustaining the extent of the second constant stress sector (CS *II*).

Further increase in pressure sensitivity magnifies these effects on the extent of stress sectors. As seen from the table for higher values of pressure sensitivity, the second constant stress sector CS *II*, which is determined by the difference (θ_B - θ_C), is almost not changed; while the centered fan sector, represented by θ_C, is reduced to less than half of its original extent.

3.2 Notch-tip Stress fields

Figure 3 shows radial and circumferential stress components, normalized by the generalized effective stress $\overline{\sigma}_0$, as functions of the angular position near the notch-tip for materials without pressure sensitivity (μ = 0), and for notch angle values of $\gamma = 0$, $\pi / 8$ and $\pi / 4$

It can be seen from the figure that the general distribution of stress fields is not changed considerably, because there is a balanced reduction in the extent of the stress sectors which determine the stress fields. We also notice a shift in locations of extreme values of stresses due to the geometry change which introduces the change in boundary conditions. Due to the reduction in the centered fan sector extent, maximum value of σ_{rr} increases with increasing notch angle.

The variation of the notch-tip stresses for materials with moderate level of pressure sensitivity ($\mu =$ 0.2 and 0.4), are plotted as functions of the angular position ahead of notch tip as shown in Figures 4 and 5, respectively, for notch angle values of $\gamma = 0$, $\pi / 8$ and $\pi / 4$. We see from the two figures that further reductions in the centered fan region extent tend to increase the radial stress. However, the counter effect resulting from the pressure sensitivity reduces this increase in radial stress.

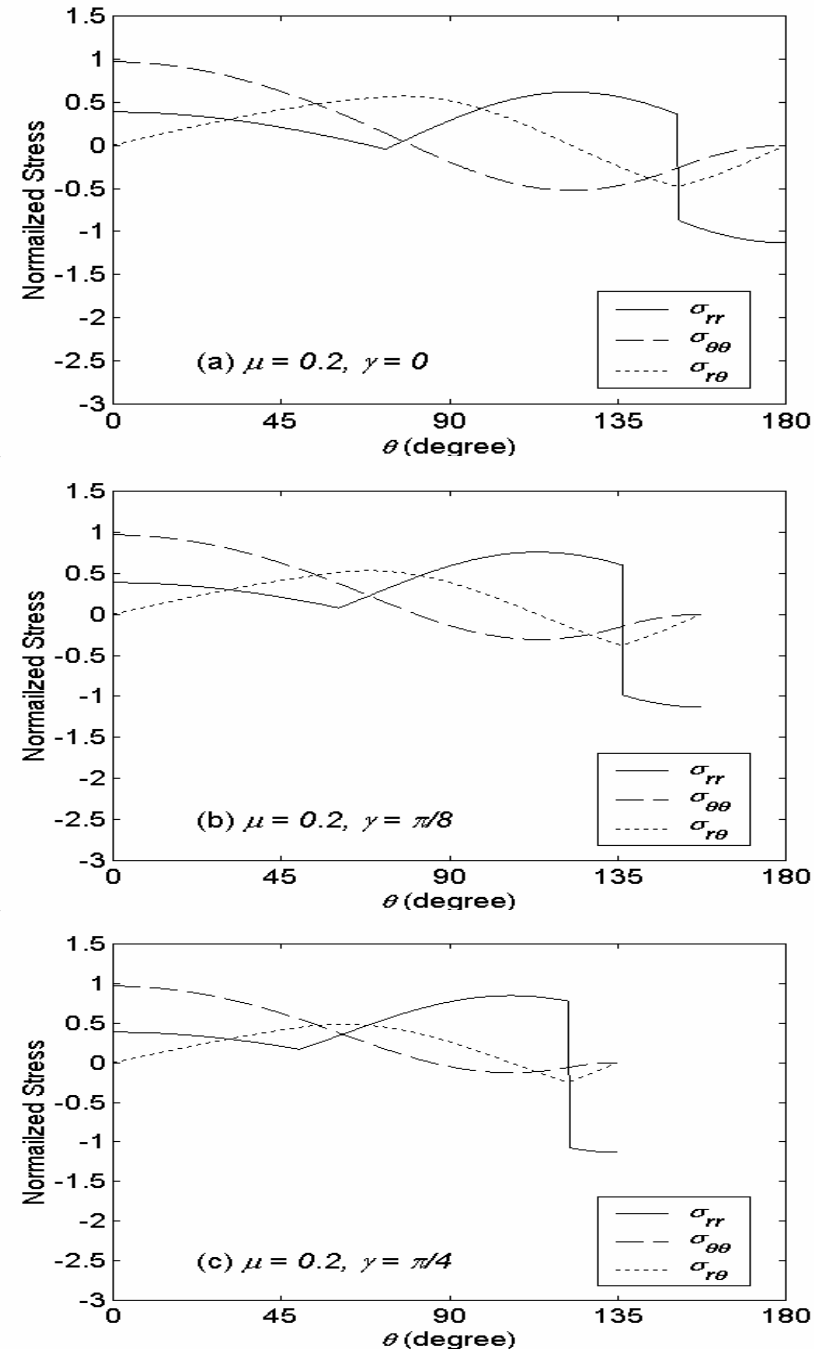

Figure 4: Angular variation of normalized stresses for a sharp notch with μ =0.2 for notch angle values of γ= 0, π/ 8 and π/ 4.

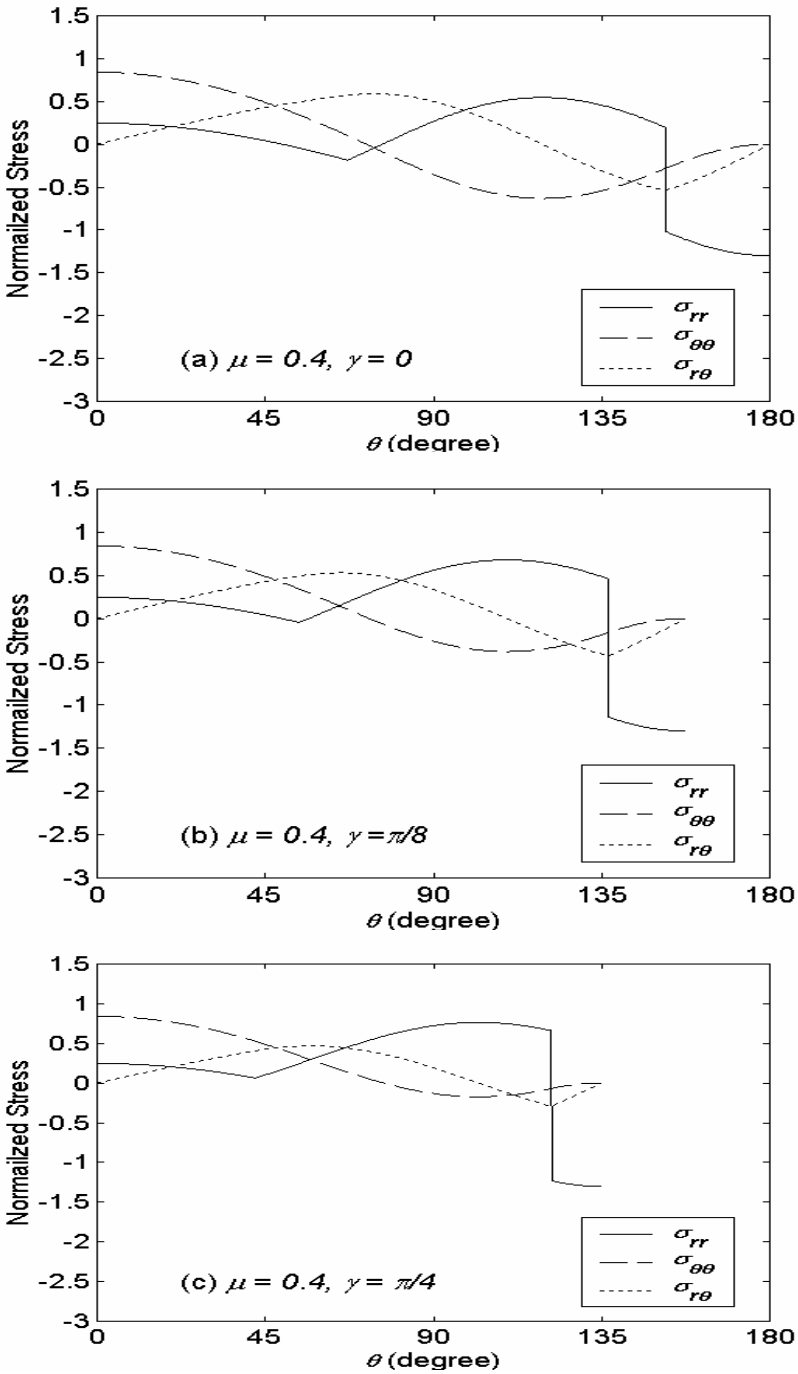

Figure 5: Angular variation of normalized stresses for a sharp notch with μ =0.4 for notch angle values of γ= 0, π/ 8 and π/ 4.

The same trend is observed in Fig. 6, which shows the angular variation of notch tip stresses for the large pressure sensitivity value of $\mu = 1.0$ for notch angle values of $\gamma = 0$, $\pi / 8$ and $\pi / 4$. In addition to previous observations for the cases discussed earlier for moderate values of pressure sensitivity, we notice a more evident effect which is the smaller variation in the stress range for all three stress components. This is due to the fact that there is a smaller span of stress distribution because of the new geometry constraint imposed by the increasing notch angle.

In all of the results discussed above, the start up case is taken with the notch angle $\gamma = 0$ representing a pure crack case, which is the problem analyzed in previous works [10, 11, 12]. Comparing the results obtained here with the results in their work, we find that there is agreement between the solutions. Moreover, the solutions presented in this work for a wedge-shaped sharp notch serve as a generalization for the pure crack case for materials with pressure sensitivity.

4. Conclusions

In this paper, the effects of notch geometry and pressure sensitivity on notch-tip fields in pressure-sensitive materials were investigated. Analytic expressions of the stress fields were presented with the notch angle dependence accounted for. This solution is a generalization for the pure crack case developed by earlier workers.

The extent of centered fan sector at notch front is reduced, which gives an increase in the radial stress value around the notch. As the pressure sensitivity increases, the reduction of the centered fan sector directly ahead of the notch tip is more evident. Also, for high pressure sensitivity values, the introduction of notch angle reduces the variation of the stress levels.

Closed-form notch-tip stress solutions obtained here are useful for design of structural components with similar geometry for materials that exhibit pressure dependent yield behavior.

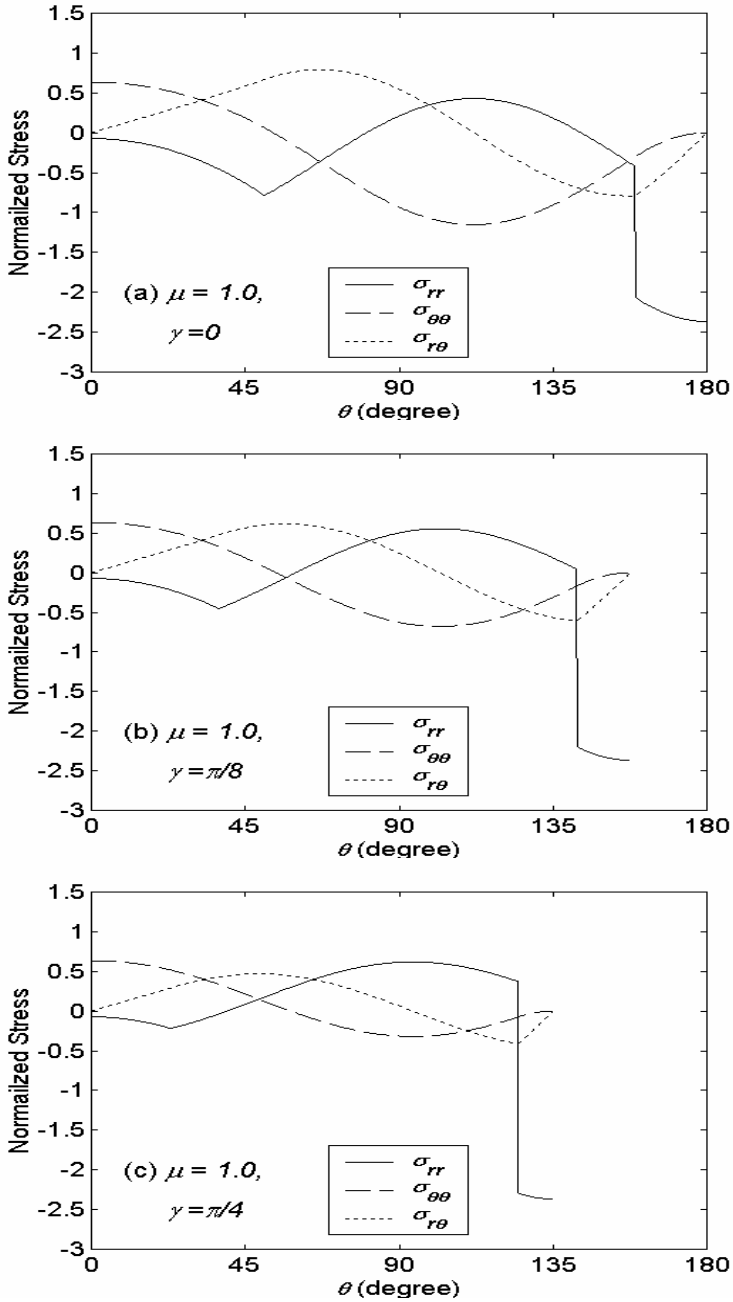

Figure 6: Angular variation of normalized stresses for a sharp notch with μ =1.0 for notch angle values of $\gamma = 0$, $\pi/8$ and $\pi/4$.

References

[1] **Sternstein, S.** and **Ongchin, L.**, Yield Criteria for Plastic Deformation of Glassy High Polymers in General Stress Fields, *American chemical Society of Polymers Preprint*, **10**, 1117-1124, (1969).

[2] **Spitzig, W.** and **Richmond**, Effect of Hydrostatic Pressure on the Deformation Behavior of Polyethylene and Polycarbonate in Tension and Compression, *Poly. Eng. Sci.*, **19**, 16, 1129-1139, (1979).

[3] **Kinloch, A.** and **Young, R.,** Fracture Behaviour of Polymers, Elsevier Applied Sciences, London**,** (1983).

[4] **Dong, M., Piour, C.** and **Francois, D.,** Damage Influence on the Fracture Toughness of Nodular Cast Iron: Part II, Damage Zone Characterization Ahead of a Crack Tip, *Metall. Mater. Trans.*, **28A**, 11, 2255-2262, (1997).

[5] **Richmond, O.** and**, Spitzig, W.**, Pressure Dependence and Dilatancy of Plastic Flow, in *International Union of Theoretical and Applied Mechanics*, (1980), 377-386.

[6] **Yu, C.** and **Chetty, D**., Transformation Zone Shape, Size, and Crack-Growth-Resistance (R-Curve) Behavior of Ceria-Partially-Stabilized Zirconia Polycrystals, *J. Amer. Ceram. Soc.*, **72**, 921-928, (1989).

[7] **Chen, I. W.,** Model of Transformation Toughening in Brittle Materials, *J Amer. Ceram.. Soc.*, **74**, 2564-2572, (1991).

[8] **Rice, J.,** and **Rosengren, G**., Plane Strain Deformation Near a Crack Tip in a Power-Law Hardening Material, *J. Mech. Phys. Solids*, **16**, 1-12, (1968).

[9] **Hutchinson, J.,** Singular Behavior at the End of a Tensile Crack in a Hardening Material, *J Mech. Phys. Solids*, **16**, 13-31, (1968).

[10] **Li, F.,** and **Pan, J,** Plane-Strain Crack-Tip Fields for Pressure-Sensitive Dilatant Materials, *J. Appl. Mech*., 57, 40-49, (1990).

[11] **Li, F.,** and **Pan, J,** Plane-Stress Crack-Tip Fields for Pressure-Sensitive Dilatant Materials, *Eng. Fract. Mech*, **35**, 6 1105-1116, (1990).

[12] **Li, F.,** The Analytic Solution of Near-Tip Stress Fields for Perfectly Plastic Pressure-Sensitive Material Under Plane Stress Condition, *Intl. J. Fract*., **53**, 325-336, (1992).

[13] **Al-Abduljabbar, A.** and **Pan, J**., Effects of Pressure Sensitivity and Notch Geometry on Notch-Tip Fields, *Poly. Eng. Sci.*, **38**, 7, 1031-1038, (1998).

[14] **Rice, J.,** Elastic-Plastic Crack Growth, In H .G. Hopkins and M. J. Sewell (eds), *Mechanics of Solids: The R. Hill 60th Anniversary Volume*, Pergamon Press, Oxford, 539-562, (1982).

[15] **Hill, R.,** Mathematical Theory of Plasticity, Clarendon Press, Oxford, (1950).

[16] **Hutchinson, J.,** Plastic Stress and Strain Fields at a Crack Tip, *J Mech. Phys. Solids*, **16,** 337-347, (1968).

حقول الإجهاد عند رؤوس الفلول الحادة للمواد ذات الليونة الحساسة للضغط لحالة الإجهاد داخل المستوي

عبدالحميد العبدالجبار

الكلية التقنية بالرياض- المملكة العربية السعودية

المستخلص: في هذا البحث، يتم إيجاد حقول الإجهاد عند رؤوس الفلول الحادة (على شكل V) للمواد ثابتة التمدد (التي يكون جهد التمدد فيها ثابتا بغض النظر عن مدى التمدد) ذات الليونة الحساسة للضغط، وذلك في حالة التحميل ذات الإجهاد داخل المستوي (ثنائي الأبعاد). وقد تم استخدام معيار دركر-براغر الرياضي للمواد ذات الحساسية لليونة لوصف خضوع المادة. وباستخدام قوانين الاتزان والشروط الحدية ومعيار الخضوع تم اشتقاق التعبيرات الرياضية لحقول الإجهاد. ويغطي البحث الارتفاع التدريجي في زاوية الفل من حالة الشق الأفقي البحت الذي تمت مقارنة نتائجه مع البحوث المنشورة مسبقا. تظهر النتائج أنه مع ازدياد مقدار زاوية الانفتاح في الفل يقل نطاق سريان الحقل المواجه لزاوية الفل خصوصا مع زيادة زاوية الفل، بالرغم من ضعف تأثر القيم المطلقة للإجهادات. كما أنه عند الحالات العالية من الحساسية للضغط فإن الزيادة في زاوية الفل تضعف مقدار التفاوت في قيم الإجهادات.